Article

Utilization of Wood Flour from White Oak Branches as Reinforcement in a Polypropylene Matrix: Physical and Mechanical Characterization

José Angel Hernández-Jiménez [1]**, Rosa María Jiménez-Amezcua** [2]**, María Guadalupe Lomelí-Ramírez** [1]**, José Antonio Silva-Guzmán** [1]**, José Guillermo Torres-Rendón** [1,]*** and Salvador García-Enriquez** [1,]***

1   Department of Wood, Cellulose and Paper, University of Guadalajara, Zapopan 45220, Mexico; jose.hernandez2610@alumnos.udg.mx (J.A.H.-J.); maria.lramirez@academicos.udg.mx (M.G.L.-R.); jantonio.silva@academicos.udg.mx (J.A.S.-G.)
2   Department of Chemical Engineering, University Guadalajara, Guadalajara 44430, Mexico; rosa.jamezcua@academicos.udg.mx
*   Correspondence: jose.torres@academicos.udg.mx (J.G.T.-R.); salvador.genriquez@academicos.udg.mx (S.G.-E.)

Abstract: Compared to other fibrous materials, plant fibers can act as a reinforcement in plastics due to their relatively high strength and rigidity, low cost, low density, biodegradability, and renewability. In this context, this study examines the effect of the particle size and content of white oak wood flour (*Quercus laeta* Liemb), obtained from its branches, on the properties of commercial polypropylene. In Mexico, wood from the branches of *Quercus laeta* Liemb is barely utilized despite its abundance and viability. The main objective of this study is to demonstrate that this waste material can be exploited to prepare useful materials, in this case composites with competitive properties. Tensile and flexural tests, as well as impact strength and melt flow index were evaluated. In addition, density and water absorption capacity were also tested. Results showed that the water absorption increased with the incorporation of wood particles. Mechanical properties were strongly influenced by particle content. A reduction in elongation and strength was observed, while Young's modulus and flexural modulus increased with the incorporation of wood particles. Impact strength increased with particle size and particle content.

Keywords: wood–plastic composites; white oak flour; polypropylene; mechanical properties; water absorption

1. Introduction

Materials used to make utensils have played a key role in the advancement of civilization. Among these materials, polymers are the ones that revolutionized the science of materials. Polymers have been used in endless applications thanks to their unique properties, versatility, lightness, and ease of processing, among other characteristics [1]. One way of use them is through mixtures with other materials, called composites, thus achieving properties that the polymer alone cannot have. An example of this is the addition of reinforcing agents [2] in polymeric matrices' plastic matrix. Such reinforcements can be glass fibers [3,4], carbon fibers [5], glass fibers/carbon nanotubes [6], kenaf [7], and Kevlar fibers [8], among others.

In recent decades, researchers have added natural fibers (cellulose-based fibers) to polymeric matrices [9], such as hemp [10,11], sugarcane bagasse [12,13], corn stalk fiber [14], jute [10,15,16], sisal [10,15,17], lino [15], rice straw stem fibers [18], henequen [19–21], agave [22–24], palm [25], coconut [26], pine cone residues [27,28], and cotton [29], among others, and were the subject of different studies such as processing methods, mechanical characterization [28], and biodegradation [30,31], among others. To improve adhesion and

mechanical properties, compatibilizers [24,32–35] and chemical modifications of natural fibers have been used [32,36–38].

Wood particles have also been used as reinforcements in polymeric matrices. This combination generates a material called wood–plastic composite or WPC. These materials have significant advantages over wood, since, in addition to being lighter, they are more resistant to humidity, have greater dimensional stability, and are resistant to biodegradation caused by insects, bacteria and fungi, mainly at low reinforcement concentrations, and therefore have longer useful lifetimes [31]. Among the materials obtained from wood that have been used are pine particles [23,31,35], maple [31], oak [31,39], oyamel [12], eucalyptus [35,40,41], poplar [42], guaje [43], and birch [44]. These materials have been used mainly in the construction and automotive industries [45,46], being of particular interest because of their great potential for synergism in mechano-static properties.

In the case of oak trees, they have been used by man since ancient times to obtain wood, food, tannins, and medicine. These plants, also known as oaks or acorns, belong to the *Quercus* genus, one of the most important worldwide [47–49]. In Mexico, oaks are considered the second most important forest resource for timber after the *Pinus* genus [49]. Oak wood has a very high value as a raw material when properly processed. However, due to its hardness, its less homogeneous geographic distribution compared to pines, and the specific variability in its technological characteristics, its most common use is still as fuel [50,51].

The *Quercus* genus is the most diverse within the Fagaceae family, distributed mainly in temperate regions and secondarily in tropical and subtropical regions of the northern hemisphere [51]. The richness of *Quercus* species is difficult to determine, but it is estimated that there may be between 300 and 600 species on the planet. In Mexico there are between 135–161 species of oaks, which makes it the holder of the largest number of species worldwide [52,53]. Nevertheless, wood utilization programs for *Quercus laeta* Liemb (an endemic species) are nonexistent in Mexico [54,55]. In particular, applications for wood from its branches are very scarce. This is mainly due to their twisted shape and lack of interest in their exploitation.

Nájera-Luna et al., reported that the density of *Quercus laeta* wood is 0.68 g/cm^3, which is classified as high. The volumetric shrinkage is 18.1%, with the tangential plane having the greatest shrinkage at 10.7%. The fiber saturation point (FSP) is established at 30.1% moisture content. The anisotropy ratio (ANR) is 1.74, classified as high, indicating low dimensional stability of the wood [56].

In this paper, we report the preparation of composites based on polypropylene (PP) and white oak wood particles (from the branches). The aim of this study is to demonstrate that wood from the branches of *Quercus laeta* Liemb can be exploited to produce wood–plastic composites with competitive properties.

2. Materials and Methods

2.1. Materials

For this work, *Quercus laeta* Liemb wood was obtained from the state of Jalisco's highlands. Indelpro brand polypropylene, an extrusion-grade homopolymer with a fluidity index of 3.8 g/10 min, and a density of 0.9 g/cm^3, was used as the thermoplastic matrix.

2.2. Wood Particles Preparation

The branches, approximately 15 cm in diameter, without bark, were reduced in size in a Bruks Mekaniska chipping machine. The chips were exposed to ambient conditions (25 °C and atmospheric pressure) to reduce humidity. A second stage of size reduction was carried out in a Plastic Pulvex grinder. Again, the lignocellulosic material was dried at ambient temperature. A particle size classification of the lignocellulosic material was carried out by retaining the particles in the meshes of a Tyler sieve, from which the particles that passed a 30 mesh were selected and then retained in the meshes 40 (594–421 μm), 50 (420–298 μm), 65 (297–211 μm) and 100 (210–150 μm).

Determination of L/D Ratio

A Leica MZ7.5 series stereomicroscope was used equipped with a $0.8 \times$ and $0.63 \times$ lens, giving a measurement field of 113.7 mm^2 with a measurement of 1 pixel = 0.0125 mm with the adapted camera. The average L/D ratio was calculated according to:

$$\lambda = \frac{\sum_{i=1}^{n} \left(\frac{L_i}{D_i} \right)}{n} \tag{1}$$

where λ is the L_i/D_i ratio average. A total of 200 wood particles were analyzed for each mesh.

2.3. Preparation of Wood-Plastic Composites

Before processing, the lignocellulosic material was dried in an oven at a temperature of 60 °C for 24 h. The mixing of polypropylene and the lignocellulosic material was carried out in a Leistritz twin-screw extruder model MICRO 27 GI/GG 32D, operating with 27 mm diameter co-rotating screws with intermeshing. The processing temperature was ramped from 170 °C to 200 °C at the extruder exit. The speed of the central screws was 260 RPM. Polymer and fiber feeding was done separately, feeding the polymer first and the fiber 30 cm later. A three-strand output die was used. Wood flour concentrations were 10 wt%, 30 wt%, and 50 wt%. Pure polypropylene was also processed, as a reference. The processed composites were pelletized and dried for 48 h at 60 °C in a temperature-controlled oven for storage and labeling. Subsequently, the pellets were used to make plates in a press (Schwabentan model Polistat 200T). The obtained materials (plates) were used to prepare samples for analysis according to ASTM standards [57–60].

2.4. Characterization of Composites

2.4.1. Water Absorption Capacity

Water absorption capacity was determined in samples with dimensions of $0.5 \times 1.0 \times 10.0 \text{ cm}^3$. These samples were first dried at 104 °C, then they were immersed in double distilled water (pH 7) in an isothermal bath at 25 °C for 4 weeks. After removing the samples from the water, they were dried on their surfaces with absorbent paper, weighed, and then put back in the water. The weight increments at different times were recorded using an electronic balance with a readability of 0.1 mg. The amount of water absorbed was calculated according to:

$$\%H = \frac{W_i - W_0}{W_0} \times 100 \tag{2}$$

where: W_i = weight of the hydrated sample at certain time, W_0 = weight of the sample at time 0. The diffusion coefficient (D) was calculated according to the method described by Cranks [61] which states that:

$$\frac{M_t}{M_\infty} = 1 - \frac{8}{\pi^2} \sum_{n=0}^{\infty} \frac{1}{(2n+1)^2} \, exp\left(-\frac{D(2n+1)^2 \pi^2 t}{l^2} \right) \tag{3}$$

where l is the thickness of the sample, M_∞ is the mass of water absorbed at equilibrium, and M_t corresponds to the mass of water absorbed at time t.

2.4.2. Melt Flow Index (MFI)

A Tinus Olsen plastometer was used to measure MFI according to ASTM D1238-13 at 190 °C [60]. In order to avoid thermal degradation of the wood flour, the lower temperature was chosen.

2.4.3. Mechanical Tests

Mechanical tensile and flexural tests were performed on a United model ASMF-100 universal testing machine, with a speed of 5.0 mm/min and equipped with a 2000 lb load cell. ASTM D638-14 [57] and ASTM D790-15e2 [58] standards were used to evaluate the

tensile and flexural properties, respectively. The operating speed on the crosshead was 4 mm/min and a 200 lb load cell was used.

The impact test was performed on a Custom Scientific Instruments, Inc. C5-126G-285 (CSI), with a free-fall dart of known weight (172 g). A total of 20 samples of each formulated composite were used. The test was performed according to ASTM D 5628-96 [59].

2.4.4. Environmental Scanning Electron Microscopy (ESEM)

Cross sections of the samples, subjected to tensile testing, were used to be observed under the ESEM microscope Hitachi model TM-1000. No pretreatment was applied to the samples.

2.4.5. Apparent Density

The apparent density was obtained using a gas pycnometer (ULTRAPYC 1200e, Quantachrome Instruments Anton Paar, Ashland, VA, USA). Nitrogen was used as the gas phase. Results are the average of five measurements.

3. Results and Discussion

3.1. Wood Particles

Table 1 shows the retention values and L/D ratio obtained for the groups of particles evaluated. The mesh with the highest quantity of retained particles was 40 (594–421 μm). The L/D ratio is very similar between the 50 and 65 meshes, with the L/D ratios of the 40 and 100 meshes being the most different from each other. The smaller particles showed a lower ratio, which could be due to shearing during the size reduction process. One of the most important parameters controlling the mechanical properties of short fiber-based composites is the fiber length or more precisely its aspect ratio (length/diameter) [62]. Maldas et al., reported the effect of wood species on the mechanical properties of wood/thermoplastic composites. They observed that differences in morphology, density, and aspect ratios between wood species explain the different reinforcing properties in thermoplastic composites [63]. Stark and Rowlands, also reported that aspect ratio, rather than particle size, has the greatest effect on strength and rigidity [64].

Table 1. Mesh type, retention and L/D ratio.

Mesh	Retention (%)	L/D Ratio
40 (594–421 μm)	35.04	4.60 ± 0.20
50 (420–298 μm)	21.62	4.32 ± 0.19
65 (297–211 μm)	16.16	4.29 ± 0.22
100 (210–150 μm)	16.95	3.93 ± 0.16

3.2. Composites

Table 2 shows that the density of the composites increases as more lignocellulosic particles are added. The density of the composites depends mainly on the content of reinforcement in the plastic matrix. The greater the amount of fiber, the higher the density of the composite.

Table 2 also shows values obtained in the melt flow index characterization, where it is observed that composites with the highest amounts of lignocellulosic particles have the lowest values. Interestingly, the particle size did not have a significant effect on the melt flow index. One could assume that having smaller particles in the system means higher MFI. However, that was not the case in our experiments. We can assume that, because of their higher superficial area, the smaller particles had more influence over the polypropylene than bigger particles at the same concentrations. A moderate resistance to flow could have been generated by this "better" integration of particles in the matrix.

Table 2. Apparent density, melt flow index, maximum water absorption, and water diffusion coefficient of samples.

Samples	Mesh and (Aspect Ratio)	Concetration of Wood Particles (wt%)	Apparent Density (g/cm^3)	Melt Flow Index (g/10 min)	Water Absortion (%)	Water Diffusion Coefficient (10^{13} m^2/s)
PP processed	-	-	0.89 ± 0.011	5.11 ± 0.14	0	-
PP-WO4010	40 (4.6 ± 0.20)	10	0.89 ± 0.010	4.17 ± 0.16	4.99 ± 0.15	2.72 ± 0.09
PP-WO4030		30	0.91 ± 0.007	1.88 ± 0.14	12.04 ± 0.48	3.03 ± 0.08
PP-WO4050		50	0.98 ± 0.019	0.91 ± 0.04	16.47 ± 0.58	4.69 ± 0.11
PP-WO5010	50 (4.32 ± 0.19)	10	0.88 ± 0.010	4.93 ± 0.13	6.71 ± 0.30	2.86 ± 0.06
PP-WO5030		30	0.92 ± 0.008	3.07 ± 0.10	8.52 ± 0.28	2.97 ± 0.07
PP-WO5050		50	0.97 ± 0.018	1.04 ± 0.03	17.25 ± 0.48	4.86 ± 0.10
PP-WO6510	65 (4.29 ± 0.22)	10	0.88 ± 0.010	4.66 ± 0.11	4.66 ± 0.18	2.56 ± 0.05
PP-WO6530		30	0.92 ± 0.007	3.18 ± 0.09	9.46 ± 0.24	3.01 ± 0.07
PP-WO6550		50	1.04 ± 0.013	1.06 ± 0.04	15.04 ± 0.47	4.08 ± 0.08
PP-WO10010	100 (3.93 ± 0.16)	10	0.91 ± 0.010	4.02 ± 0.12	1.90 ± 0.06	2.26 ± 0.05
PP-WO10030		30	0.92 ± 0.008	2.23 ± 0.08	9.429 ± 0.37	3.03 ± 0.08
PP-WO10050		50	1.07 ± 0.014	1.07 ± 0.04	12.57 ± 0.33	3.61 ± 0.7

Sample identification: PP-WOXXYY where XX or XXX is the mesh in which wood particles were retained and YY is the concentration of particles in the composite.

The maximum water absorption values, displayed in Table 2, show that water absorption increased with quantity. It can also be observed that when the aspect ratio decreased, water absorption decreased as well. This could be attributed to a better fiber–matrix adhesion. Physicochemical equilibrium was reached after two weeks of immersion in distilled water (Figure 1). Experimentally, no changes in dimensions or deformation of samples was observed. Nájera-Luna et al., reported that the saturation point of white oak fiber was 30.1% moisture content [56]. Water absorption in WPCs is an important quality indicator because these materials absorb less moisture and do so more slowly than wood. WPCs are more resistant to fungal decay and have better dimensional stability when exposed to humidity [31,63,65]. Water absorption capacity is affected by the nature of the wood particles and the thermoplastic matrix [66]. Ideally, the polymer completely covers the wood particles, preventing contact between them and with the outside. The actual process involves contact between the wood particles, as well as the surface particles with the outside, so the rate of water absorption is very slow, due to the fact that the internal wood particles absorb water only by capillarity. The diffusion coefficient increases with the amount of wood particles, the values of the coefficients varied from 2.26×10^{-13} to 4.69×10^{-13}, which corresponds to the composites that absorbed the least and most water, PP-WO10010 and PP-WO5050, respectively. Mishra, and Verma [67], and Tajvidi et al. [68], suggested that this is due to the increase in the number of free OH groups of cellulose contained in the fiber. These free OH groups come into contact with water and form hydrogen bonds, resulting in an increase in weight in the composite material.
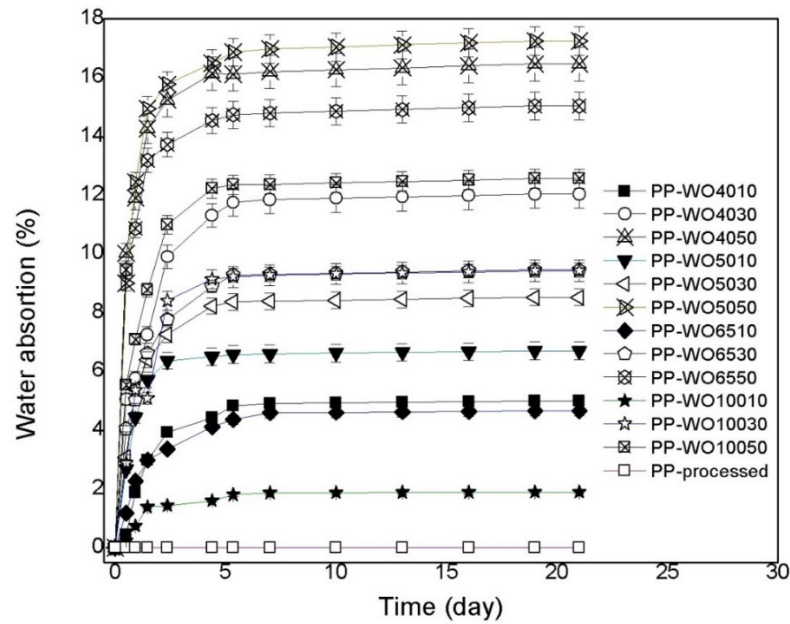
Figure 1. Water absorption kinetics for all the composites evaluated.

3.3. Impact Tests

The effect of particle concentration is presented in Figure 2, where it is observed that the higher the concentration of lignocellulosic particles, the greater the energy required to cause a failure. This effect is greater for the particle sizes retained in 40 and 100 mesh, with the latter having a higher value. The closest value to processed polypropylene (PP) belongs to composites having particles retained in the 100 mesh at 50 wt%. In composites having 10 wt% and 30 wt% of wood fibers, samples with particles with the highest aspect ratios (from particles of meshes 65 and 100) needed more energy to reach rupture. However, in composites with 50 wt% of fibers, samples that had the highest and lowest aspect ratios (from particles of meshes 100 and 40 respectively) were the ones with the better bending stress. It is possible that composites having 50 wt% of particles (from the mesh 40) had fibers oriented in a certain manner (perpendicular to the direction of the impact) that increased their bending strength. Ashori, determined that the impact resistance of PP increases when combined with wood fibers in proportions between 10 and 40 wt% [63]. The impact properties of composites are usually directly related to hardness, which is influenced by the nature of the constituent materials and the fiber–matrix interface [69]. Nourbakhsh and Ashori, worked with compositions between 10 wt% and 40 wt% black poplar wood particles and found that higher impact strength is obtained with the 10 wt% concentration [70].
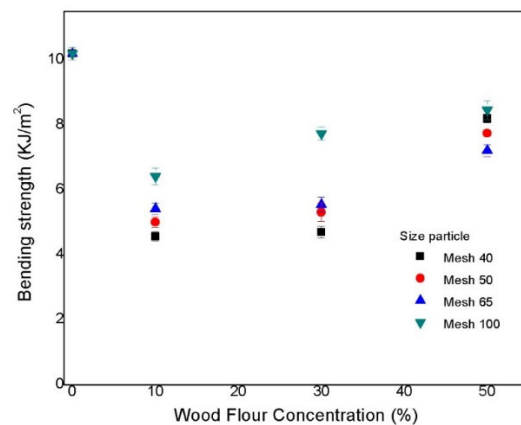

Figure 2. Bending strength as a function of wood particle content.

3.4. Flexion Tests

Figure 3 shows the effect of incorporating white oak lignocellulosic particles in the polypropylene matrix. At higher particle concentrations, the flexural strength increased for composites having particles retained in the 100 mesh, followed by those containing particles retained in the 40 mesh, while the increase for the 40 mesh particle size was at lower concentration. Figure 3 shows the behavior of the flexural modulus for all the composites evaluated. It was observed that the higher the particle concentration, the higher the flexural modulus increases for the composites containing reinforcements retained in the 100 mesh, followed by those with particles retained in the 40 mesh. On the other hand, the lower the particle concentration, the higher the value of this parameter in composites having wood flour retained in the 40 mesh. In general, the bending modulus is significantly affected by the particle quantity and not so much by the size. The aspect ratio of the fibers did not have any clear relationship with the flexural modulus. It is possible that other factors, such as the orientation of the fibers, trumped the effect of this fiber characteristic. It is worth mentioning that in this test a perpendicular force is applied to the sample and the geometry of the lignocellulosic particles has a direct influence. Since their lengths are greater than their diameters, the particles that are axially oriented presented resistance to bending which improves the flexural modulus in the polymeric matrix.
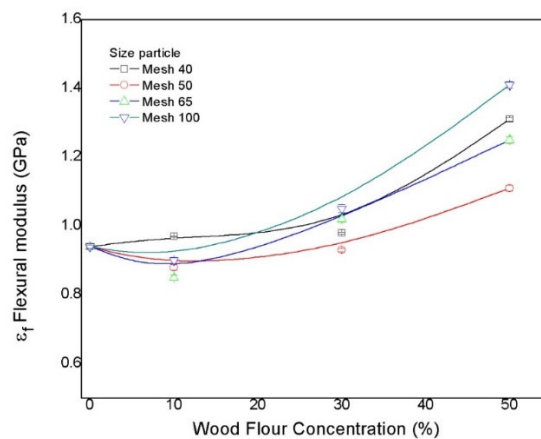

Figure 3. Flexural modulus as a function of particle content.

3.5. Tensile Tests

Table 3 shows the values of tensile properties, Young's modulus, ultimate tensile strength and elongation at break. Young's modulus is affected by the addition of ligno-cellulosic particles (Figure 4a). In most composites, as the amount of particles increases, Young's modulus increases, which means that they become stiffer. In general, as the particle size decreased, Young's modulus increased for composites with 10 wt% and 50 wt% of reinforcement. The values reported in this work are consistent with those reported by Ichazo et al., for PP/WF (mixture of mahogany cedar, pine, oak, and saki-saki) composites [71]. Nair, Diwan, and Thomas, proposed that if the fibers are oriented perpendicular to the crack propagation direction, the crack may be obstructed, and this explains the increase in modulus [72].

When lignocellulosic particles are added, the ultimate tensile strength decreases for all particle sizes, obtaining the lowest values for 50 wt% concentration in PP-WO10050 composites (Figure 4b). In general, as the concentration increases and the oak wood particle size decreases, the ultimate tensile strength decreases due to the increase in area for a given mass, which generates a greater amount of interface between the lignocellulosic particles and the polymeric matrix. The values reported in this work are consistent with those reported by Ichazo et al., for PP/WF composites [71].

Table 3. Mechanical properties of composites.

Formulations	Impact	Flexural		Tensile		
	Bending Strength (KJ/m^2)	σ_f Maximum Strength (MPa)	ε_f Flexural Modulus (GPa)	σ_t Ultimate Tensile Strength (MPa)	Elongation at Break (%)	ε_t Young's Modulus (GPa)
PP processed	10.2 ± 0.20	40.03 ± 0.98	0.94 ± 0.005	26.80 ± 1.08	420 ± 10.5	1.73 ± 0.04
PP-WO4010	4.57 ± 0.15	39.03 ± 1.71	0.97 ± 0.002	19.35 ± 1.27	1.49 ± 0.04	1.54 ± 0.01
PP-WO4030	4.70 ± 0.18	32.42 ± 0.34	0.98 ± 0.003	16.79 ± 0.90	1.14 ± 0.03	2.52 ± 0.02
PP-WO4050	8.20 ± 0.13	35.25 ± 0.45	1.31 ± 0.006	11.22 ± 0.41	0.71 ± 0.01	2.73 ± 0.03
PP-WO5010	5.01 ± 0.16	32.2 ± 1.14	0.88 ± 0.008	19.78 ± 1.22	1.69 ± 0.05	1.70 ± 0.01
PP-WO5030	5.32 ± 0.28	31.49 ± 1.01	0.93 ± 0.005	18.64 ± 1.41	1.16 ± 0.03	2.44 ± 0.02
PP-WO5050	7.75 ± 0.09	28.13 ± 0.90	1.11 ± 0.009	9.85 ± 0.47	0.62 ± 0.01	2.68 ± 0.02
PP-WO6510	5.42 ± 0.17	32.34 ± 1.05	0.85 ± 0.008	19.42 ± 1.08	1.71 ± 0.03	1.42 ± 0.02
PP-WO6530	5.55 ± 0.23	33.66 ± 0.61	1.02 ± 0.009	13.2 ± 0.67	1.06 ± 0.02	1.96 ± 0.06
PP-WO6550	7.21 ± 0.18	35.45 ± 0.41	1.25 ± 0.010	9.12 ± 0.45	0.48 ± 0.01	2.54 ± 0.02
PP-WO10010	6.42 ± 0.26	34.56 ± 0.55	0.90 ± 0.009	17.56 ± 0.92	1.38 ± 0.03	1.76 ± 0.01
PP-WO10030	7.74 ± 0.20	32.68 ± 0.23	1.05 ± 0.012	14.88 ± 0.93	1.11 ± 0.03	1.98 ± 0.03
PP-WO10050	8.46 ± 0.29	39.10 ± 0.48	1.41 ± 0.009	8.21 ± 0.40	0.52 ± 0.01	2.60 ± 0.03

Elongation at break is affected by the incorporation of particles, as can be seen in Figure 4c. As the number of particles increases, elongation at break decreases, independently of the particle size. The smallest elongations at break occurred for the PP-WO6550 composite. In general, the maximum elongation tends to decrease with increasing concentration. No clear effects on the tensile parameters from the size and aspect ratio of the wood particles were identified. It seems that other factors overshadowed the effect that these particle characteristics could have had over the tensile mechanical properties. One of these factors could be the orientation of the wood particles, which at the moment we cannot fully control. Wood is known for having anisotropic mechanical properties, which can greatly influence the tensile mechanical properties of the material that contains them [73].

Table 3 shows the mechanical properties of all composites evaluated. Fiber concentration is the factor that has the strongest effect on mechanical properties. Table 4 displays several studies dealing with polypropylene-based WPCs having lignocellulosic materials as reinforcements. It is important to mention that direct comparison of the mechanical properties of such composites is difficult, since those properties greatly depend on many factors, such as the preparation method and characteristics of reinforcements such as their size, morphology and chemical composition. Also, the type of polypropene, concentration of components, orientation of reinforcements and presence of coupling agents have a considerable impact. From Table 4 it is clear that our composites have comparable properties with other similar PP/oak-based composites reported [74,75]. It is important to notice that those composites were prepared with other oak species. Our composites had the highest Young's modulus (2730 MPa) but at a higher concentration of fibers (50 wt%) compared to the other PP/oak composites (~2050 MPa with 40 wt% and ~790 Mpa with 30 wt%). Interestingly, only three types of composites, the ones containing pine, eucalyptus and olive stones, reported higher Young´s modulus values than ours, which demonstrates the competitiveness of our composites. In the case of the tensile strength, we have a slightly below average value compared to those reported by the rest, including the two PP/oak studies. This is expected since in theory our material is one of the most brittle. Moreover, our values of flexural modulus and flexural strength are comparable to those from all composites included in Table 4.
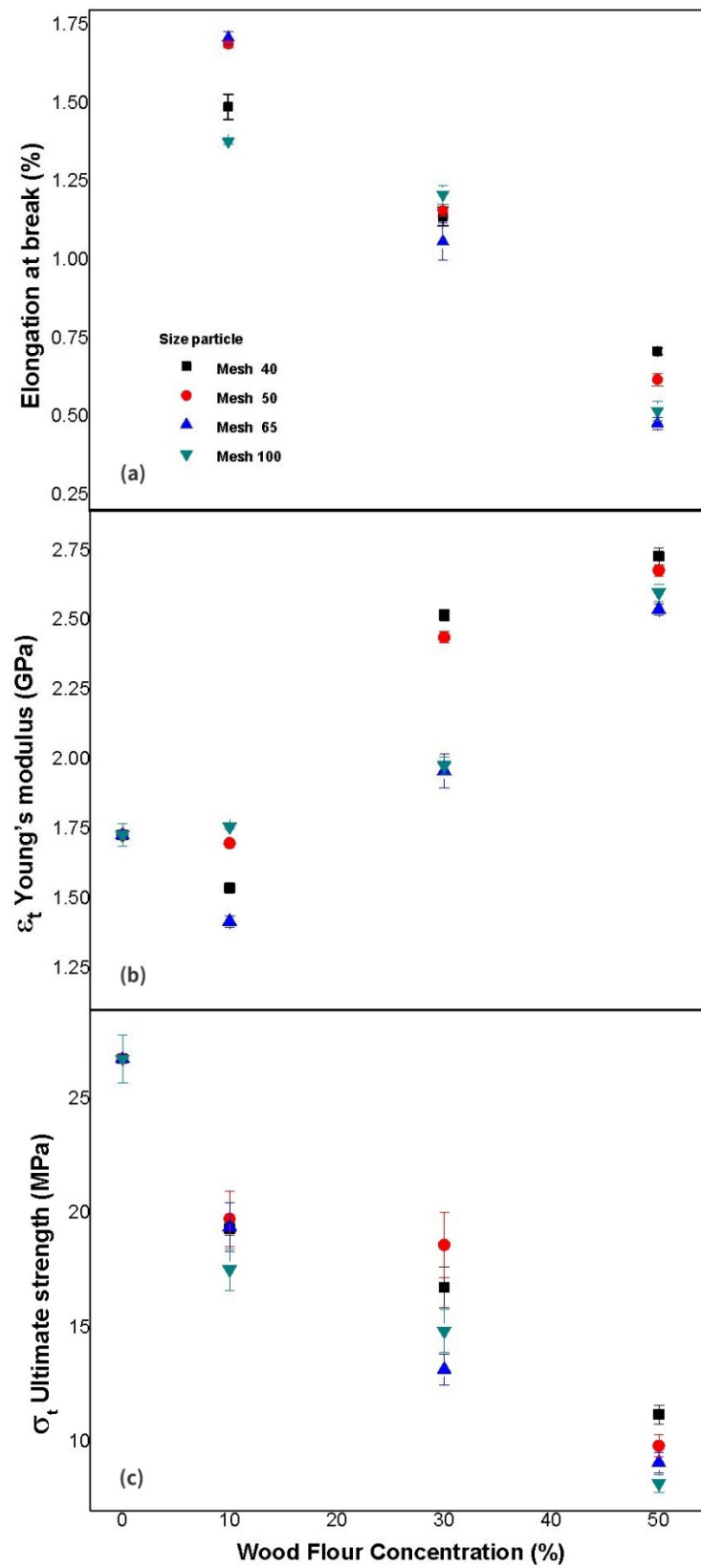
Figure 4. Mechanical properties of tensile tests: (**a**) Young's modulus, (**b**) ultimate tensile strength, and (**c**) elongation at break as functions of particle size and concentration.

Table 4. Mechanical properties of polypropylene (PP)-based composites reinforced with lignocellulosic materials.

Fiber/Particle	Composition			Mechanical Properties				References
	Fiber/ Particle (wt%)	C.a.*	PP (wt%)	Tensile Modulus (MPa)	Tensile Strength (MPa)	Flexural Strength (MPa)	Flexural Modulus (MPa)	
Poplar (Alamo)	30		70	~1230 **			~1300 *	Ashori 2009 [62]
Agave	30		70	~600 **	23.5 ± 0.1	43.3 ± 1.8	1632.62	Perez-Fonseca et al., 2014 [23]
Agave	30		70	2221± 60.4	23.2 ± 0.43	39.2 ± 0.53	1176 ± 36.3	Langhorst et al., 2018 [46]
Birch	20		80	~1080 **	~17 **			Kakroodi et al. 2012 [44]
	40		60	~1290 **	~15.5 **			
Eucalyptus	40		60	~3800 **	~22.8 **		~2600 **	Maziero et al., 2019 [35]
Coir fibers and oil palm	30		70	~2134	~30.851	~53.012	~2920	Zainudin et al., 2014 [26]
Cotton strands	30		70		38.2			Serra et al., 2017 [29]
	40		60		41.7			
Jute	10		90		20.60	27.61		Mohanty et al., 2004 [32]
	15		85		21.67	32.63		
	30		70		24.20	34.31		
Oak (Quercus castaneifolia)	40	2	60	~2050 **	~24 *	~31 **	~2350 **	Ashori and Nourbakhsh, 2010 [75]
Oak (Quercus pedunculata L.)	30		70	~790	~26			Borysiak and Paukszta, 2008 [74]
Oak (Quercus Laeta Liemb)	10–50		90–50	1420–2730	9.12–19.42	28.13–39.10	850–1410	Our Work
Olive stones	30		70	~3450 **	~24			Naghmouchi et al., 2015 [34]
Palm	5	2	93			24.4 ± 0.9	783.7 ± 83.6	Goulart et al., 2011 [25]
Pine and beech	40	3	57			48.1 ± 2.17	5005.2 ± 109.4	Ayrilmis et al., 2010 [27]
Pine	40		60	~3100 *	~21.3 **		~2550 **	Maziero et al., 2019 [35]
Pine	30		70	~620 **	28.0 ± 1.0	46.2 ± 2.0	1427 ± 41	Perez-Fonseca et al., 2014 [23]
Pine	40		60	3200–3610	21.7–25.5	38.7–42.9	2690–3150	Stark and Rowland, 2003 [64]
Pine	40	2	60	~1750 **	~19 **	~27 **	~2000 **	Ashori and Nourbakhsh, 2010 [75]
Pine	30		70	~750	~24			Borysiak and Paukszta, 2008 [74]
Sugar cane bagasse	20		80	1442.5 ± 68.7	22.3 ± 0.8	37.2 ± 2.1	960.7 ± 139.2	Cerqueira et al., 2011 [12]
	10		90	1027.1 ± 82.9	23.0 ± 0.6	35.5 ± 3.6	1200.8 ± 112.9	

* Coupling agent. ** Estimation of the value (from Figures).

3.6. Scanning Electron Microscopy (SEM)

According to the obtained SEM images, composites having 10 wt% of wood particles with the larger (PP-WO4010) and smaller wood particles (PP-WO10010) within are shown in Figure 5a,c, respectively. The PP-WO4010 samples showed uniform distribution throughout the polymer matrix. In both images, a single wood particle can be observed immersed in a plastic matrix with apparent adhesion at the wood–polymer interface as expected for a low wood particle concentration. SEM images Figure 5b,d, show the composites made with the highest wood particle content (50 wt%) containing the largest and smallest particles, respectively (PP-WO4050 and PP-WO10050). No adhesion failure is evident at

the wood–plastic interface. However, the particles tend to agglomerate into larger clusters of uneven, non-directional distribution and at a considerable distance from each other. It is because of these large gaps between the clusters that the impact flexural strength is reduced in this type of composite, as the dynamic load resistance is largely dictated by the weaker polymer with little participation of the stronger wood filler.
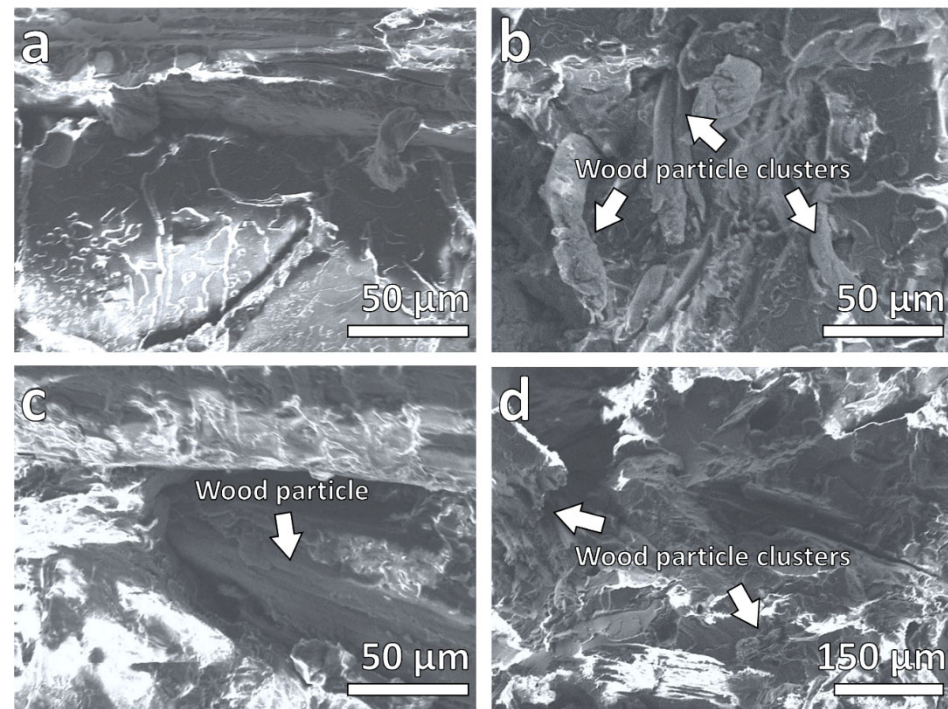

Figure 5. SEM micrographs of fracture surfaces of (**a**) PP-WO4010, (**b**) PP-WO4050, (**c**) PP-WO10010, and (**d**) PP-WO10050 composites.

4. Conclusions

According to the results, it is feasible to use wood from the branches of *Quercus laeta* Liemb to obtain wood–plastic composites at different concentrations and wood particle sizes. The index flow rate was affected mainly by the percentage of lignocellulosic particles: the higher the percentage, the lower the flow rate. The rupture energy in the impact test was affected mainly by the concentration of lignocellulosic particles: the greater the amount, the more energy is needed to have a failure. Likewise, the larger the particle size, the lower the bending strength. The flexural strength and flexural modulus increased for particles retained in the 40 and 100 meshes at a concentration of 50 wt%. The flexural modulus increased as the concentration of particles increased. Young's modulus, ultimate tensile strength, and elongation at break were directly affected by the presence of lignocellulosic particles: as the percentage of wood particles increased, elongation at break decreased, and ultimate tensile strength and Young's modulus increased. Composites with the best properties (less brittleness and higher mechanical properties, lower water absorption) were found at a percentage of 30 wt% of particles retained in the 50 to 65 mesh.

Author Contributions: Conceptualization, J.G.T.-R. and S.G.-E.; methodology, J.A.H.-J., R.M.J.-A., and S.G.-E.; validation, M.G.L.-R., J.A.S.-G. and S.G.-E.; formal analysis, J.A.H.-J. and J.G.T.-R.; investigation, M.G.L.-R., J.A.S.-G. and S.G.-E.; resources, R.M.J.-A., J.A.S.-G., J.G.T.-R. and S.G.-E.; data curation, J.A.H.-J. and J.G.T.-R.; writing—original draft preparation, R.M.J.-A., J.G.T.-R. and S.G.-E.; writing—review and editing, R.M.J.-A., J.G.T.-R. and S.G.-E.; visualization, J.G.T.-R. and S.G.-E.; supervision, J.G.T.-R. and S.G.-E.; project administration, J.G.T.-R. and S.G.-E.; funding acquisition, J.A.S.-G., J.G.T.-R. and S.G.-E. All authors have read and agreed to the published version of the manuscript.

References

1. Jang, B.Z. *Advanced Polymer Composites: Principles and Applications*; ASM International: Materials Park, OH, USA, 1994; p. 305.
2. Clyne, T.; Hull, D. *An Introduction to Composite Materials*, 2nd ed.; Cambridge Solid State Science Series; Cambridge University Press: Cambridge, UK, 2019.
3. Karian, H. Mega-Coupled Polypropylene Composites of Glass Fibers. In *Handbook of Polypropylene and Polypropylene Composites*, 2nd ed.; Revised and Expanded; CRC Press: Boca Raton, FL, USA, 2003. [CrossRef]
4. Fang, J.; Zhang, L.; Li, C. The combined effect of impregnated rollers configuration and glass fibers surface modification on the properties of continuous glass fibers reinforced polypropylene prepreg composites. *Compos. Sci. Technol.* **2020**, *197*, 108259. [CrossRef]
5. Choi, W.K.; Kim, H.I.; Kang, S.J.; Lee, Y.S.; Han, J.H.; Kim, B.J. Mechanical interfacial adhesion of carbon fibers-reinforced polarized-polypropylene matrix composites: Effects of silane coupling agents. *Carbon Lett.* **2016**, *17*, 79–84. [CrossRef]
6. Rasana, N.; Jayanarayanan, K.; Pavithra, R.; Nandhini, G.R.; Ramya, P.; Veeraraagavan, A.V. Mechanical and thermal properties modeling, sorption characteristics of multiscale (multiwalled carbon nanotubes/glass fiber) filler reinforced polypropylene composites. *J. Vinyl Addit. Technol.* **2019**, *25*, E94–E107. [CrossRef]
7. Karnani, R.; Krishnan, M.; Narayan, R. Biofiber-reinforced polypropylene composites. *Polym. Eng. Sci.* **1997**, *37*, 476–483. [CrossRef]
8. Fu, S.; Yu, B.; Tang, W.; Fan, M.; Chen, F.; Fu, Q. Mechanical properties of polypropylene composites reinforced by hydrolyzed and microfibrillated Kevlar fibers. *Compos. Sci. Technol.* **2018**, *163*, 141–150. [CrossRef]
9. Malkapuram, R.; Kumar, V.; Negi, Y.S. Recent development in natural fiber reinforced polypropylene composites. *J. Reinf. Plast. Compos.* **2009**, *28*, 1169–1189. [CrossRef]
10. Mwaikambo, L.Y.; Ansell, M.P. Chemical modification of hemp, sisal, jute and kapok fibers by alkalization. *J. Appl. Polym. Sci.* **2002**, *84*, 2222–2234. [CrossRef]
11. Badji, C.; Beigbeder, J.; Garay, H.; Bergeret, A.; Bénézet, J.C.; Desauziers, V. Under glass weathering of hemp fibers reinforced polypropylene biocomposites: Impact of Volatile Organic Compounds emissions on indoor air quality. *Polym. Degrad. Stab.* **2018**, *149*, 85–95. [CrossRef]
12. Cerqueira, E.F.; Baptista, C.A.R.P.; Mulinari, D.R. Mechanical behaviour of polypropylene reinforced sugarcane bagasse fibers composites. *Procedia Eng.* **2011**, *10*, 2046–2051. [CrossRef]
13. Lila, M.K.; Singhal, A.; Banwait, S.S.; Singh, I. A recyclability study of bagasse fiber reinforced polypropylene composites. *Polym. Degrad. Stab.* **2018**, *152*, 272–279. [CrossRef]
14. Ashori, A.; Nourbakhsh, A.; Tabrizi, A.K. Thermoplastic hybrid composites using bagasse, corn stalk and E-glass fibers: Fabrication and characterization. *Polym. Technol. Eng* **2014**, *53*, 1–8. [CrossRef]
15. Jayaraman, K. Manufacturing sisal–polypropylene composites with minimum fibre degradation. *Compos. Sci. Technol.* **2003**, *63*, 367–374. [CrossRef]
16. Uawongsuwan, P.; Yang, Y.; Hamada, H. Long jute fiber-reinforced polypropylene composite: Effects of jute fiber bundle and glass fiber hybridization. *J. Appl. Polym. Sci.* **2015**, *132*, 41819. [CrossRef]
17. Bassyouni, M. Dynamic mechanical properties and characterization of chemically treated sisal fiber-reinforced polypropylene biocomposites. *J. Reinf. Plast. Compos.* **2018**, *37*, 1402–1417. [CrossRef]
18. Jayamani, E.; Hamdan, S.; Rahman, M.R.; Bakri, M.K.B. Study of sound absorption coefficients and characterization of rice straw stem fibers reinforced polypropylene composites. *Bioresources* **2015**, *10*, 3378–3392. [CrossRef]
19. Herrera-Franco, P.; Valadez-Gonzalez, A.; Cervantes-Uc, M. Development and characterization of a HDPE -sand- natural fiber composite. *Compos. B Eng.* **1997**, *28*, 331–343. [CrossRef]
20. Lee, H.S.; Cho, D.; Han, S.O. Effect of natural fiber surface treatments on the interfacial and mechanical properties of henequen/polypropylene biocomposites. *Macromol. Res.* **2008**, *16*, 411–417. [CrossRef]
21. Tarrés, Q.; Vilaseca, F.; Herrera-Franco, P.J.; Espinach, F.X.; Delgado-Aguilar, M.; Mutjé, P. Interface and micromechanical characterization of tensile strength of bio-based composites from polypropylene and henequen strands. *Ind. Crops Prod.* **2019**, *132*, 319–326. [CrossRef]

22. Gómez, D.M.; Galindo, J.R.; González, N.R.; Rodrigue, D. Polymer composite based on agave fibres. In Proceedings of the Conference Proceedings: ANTEC 2005, Hynes Convention Center, Boston, MA, USA, 1–5 May 2005; p. 1346.

23. Pérez-Fonseca, A.A.; Robledo-Ortíz, J.R.; Moscoso-Sánchez, F.J.; Rodrigue, D.; González-Núñez, R. Injection molded self-hybrid composites based on polypropylene and natural fibers. *Polym. Compos.* **2014**, *35*, 1798–1806. [CrossRef]

24. Sanjuan-Raygoza, R.J.; Jasso-Gastinel, C.F. Effect of waste agave fiber on the reinforcing of virgin or recycled polypropylene. *Rev. Mex. Ing. Quim.* **2009**, *8*, 319–327. Available online: http://www.scielo.org.mx/scielo.php?script=sci_arttext&pid=S1665-273820 09000300011&lng=es&nrm=iso (accessed on 2 March 2022).

25. Goulart, S.A.S.; Oliveira, T.A.; Teixeira, A.; Miléo, P.C.; Mulinari, D.R. Mechanical behaviour of polypropylene reinforced palm fibers composites. *Procedia Eng.* **2011**, *10*, 2034–2039. [CrossRef]

26. Zainudin, E.S.; Yan, L.H.; Haniffah, W.H.; Jawaid, M.; Alothman, O.Y. Effect of coir fiber loading on mechanical and morphological properties of oil palm fibers reinforced polypropylene composites. *Polym. Compos.* **2014**, *35*, 1418–1425. [CrossRef]

27. Ayrilmis, N.; Buyuksari, U.; Dundar, T. Waste pine cones as a source of reinforcing fillers for thermoplastic composites. *J. Appl. Polym. Sci.* **2010**, *117*, 2324–2330. [CrossRef]

28. Messaoudi, K.; Nekkaa, S.; Guessoum, M. Contribution of surface treatments by esterification and silanization in reinforcing the composites based on Pine cone and Spartium junceum flours and polypropylene. *J. Adhes. Sci. Technol.* **2019**, *33*, 2405–2429. [CrossRef]

29. Serra, A.; Tarrés, Q.; Claramunt, J.; Mutjé, P.; Ardanuy, M.; Espinach, F.X. Behavior of the interphase of dyed cotton residue flocks reinforced polypropylene composites. *Compos. B Eng.* **2017**, *128*, 200–207. [CrossRef]

30. Verhey, S.; Lank, P.; Richter, D. Laboratory decay resistance of woodfiber/thermoplastic composites. *For. Prod. J.* **2001**, *51*, 44.

31. Lomelí-Ramírez, M.G.; Ochoa-Ruiz, H.G.; Fuentes-Talavera, F.J.; García-Enriquez, S.; Cerpa-Gallegos, M.A.; Silva-Guzmán, J.A. Evaluation of accelerated decay of wood plastic composites by Xylophagus fungi. *Int. Biodeterior. Biodegrad.* **2009**, *63*, 1030–1035. [CrossRef]

32. Mohanty, S.; Nayak, S.K.; Verma, S.K.; Tripathy, S.S. Effect of MAPP as a Coupling Agent on the Performance of Jute–PP Composites. *J. Reinf. Plast. Compos.* **2004**, *23*, 625–637. [CrossRef]

33. Nourbakhsh, A.; Ashori, A.; Tabari, H.Z.; Rezaei, F. Mechanical and thermo-chemical properties of wood-flour/polypropylene blends. *Polym. Bull.* **2010**, *65*, 691–700. [CrossRef]

34. Naghmouchi, I.; Espinach, F.X.; Mutjé, P.; Boufi, S. Polypropylene composites based on lignocellulosic fillers: How the filler morphology affects the composite properties. *Mater. Des.* **2015**, *65*, 454–461. [CrossRef]

35. Maziero, R.; Soares, K.; Itman Filho, A.; Júnior, A.R.F.; Rubio, J.C.C. Maleated Polypropylene as Coupling Agent for Polypropylene Composites Reinforced with Eucalyptus and Pinus Particles. *Bioresources* **2019**, *14*, 4774–4791. [CrossRef]

36. Joseph, K.; Thomas, S.; Pavithran, C. Effect of chemical treatment on the tensile properties of short sisal fibre-reinforced polyethylene composites. *Polymer* **1996**, *37*, 5139–5149. [CrossRef]

37. Sreekala, M.S.; Kumaran, M.G.; Joseph, S.; Jacob, M.; Thomas, S. Oil palm fibre reinforced phenol formaldehyde composites: Influence of fibre surface modifications on the mechanical performance. *Appl. Compos. Mater.* **2000**, *7*, 295–329. [CrossRef]

38. Cisneros-López, E.O.; Anzaldo, J.; Fuentes-Talavera, F.J.; González-Núñez, R.; Robledo-Ortíz, J.R.; Rodrigue, D. Effect of agave fiber surface treatment on the properties of polyethylene composites produced by dry-blending and compression molding. *Polym. Compos.* **2017**, *38*, 96–104. [CrossRef]

39. Flores-Hernández, M.A.; González, I.; Lomelí-Ramírez, M.G.; Fuentes-Talavera, F.J.; Silva-Guzmán, J.A.; Cerpa-Gallegos, M.A.; García-Enriquez, S. Physical and mechanical properties of wood plastic composites polystyrene-white oak wood flour. *J. Compos. Mater.* **2014**, *48*, 209–217. [CrossRef]

40. Melo, B.N.; Pasa, V.M. Composites based on eucalyptus tar pitch/castor oil polyurethane and short sisal fibers. *J. Appl. Polym. Sci.* **2003**, *89*, 3797–3802. [CrossRef]

41. Flores-Hernández, M.Á.; Torres-Rendón, J.G.; Jiménez-Amezcua, R.M.; Lomelí-Ramírez, M.G.; Fuentes-Talavera, F.J.; Silva-Guzmán, J.A.; García-Enriquez, S. Studies on Mechanical Performance of Wood-Plastic Composites: Polystyrene-Eucalyptus globulus Labill. *Bioresources* **2017**, *12*, 6392–6404. [CrossRef]

42. Costa, T.H.; Carvalho, D.L.; Souza, D.C.; Coutinho, F.M.; Pinto, J.C.; Kokta, B.V. Statistical experimental design and modeling of polypropylene–wood fiber composites. *Polym. Test.* **2000**, *19*, 419–428. [CrossRef]

43. Granda, L.A.; Espinach, F.X.; López, F.; García, J.C.; Delgado-Aguilar, M.; Mutjé, P. Semichemical fibres of Leucaena collinsii reinforced polypropylene: Macromechanical and micromechanical analysis. *Compos. B Eng.* **2016**, *91*, 384–391. [CrossRef]

44. Kakroodi, A.R.; Leduc, S.; González-Núñez, R.; Rodrigue, D. Mechanical Properties of Recycled Polypropylene/SBR Rubber Crumbs Blends Reinforced by Birch Wood Flour. *Polym. Polym. Compos.* **2012**, *20*, 439–444. [CrossRef]

45. Dahlke, B.; Larbig, H.; Scherzer, H.D.; Poltrock, R. Natural fiber reinforced foams based on renewable resources for automotive interior applications. *J. Cell. Plast.* **1998**, *34*, 361–379. [CrossRef]

46. Langhorst, A.E.; Burkholder, J.; Long, J.; Thomas, R.; Kiziltas, A.; Mielewski, D. Blue-agave fiber-reinforced polypropylene composites for automotive applications. *Bioresources* **2018**, *13*, 820–835. [CrossRef]

47. Mass, P.J. Los encinos como fuente potencial de madera para celulosa y papel en México. *Rev. Mex. Cienc. For.* **1977**, *9*, 39–58.

48. Bonfil, C. La riqueza de los encinos. *Ciencias* **1993**, *29*, 13–16. Available online: http://revistas.unam.mx/index.php/cns/article/viewFile/11329/10654 (accessed on 5 October 2021).

49. Challenger, A. *Utilización y Conservación de los Ecosistemas Terrestres de México. Pasado, Presente y Futuro (No. 581.5 C44Y)*; Comisión Nacional para el Conocimiento y Uso de la Biodiversidad: México, D.F., Mexico, 1998.

50. Nixon, K.C. The genus Quercus in Mexico. In *Biological diversity of Mexico: Origins and Distribution*; Ramamoorthy, T.P., Bye, R., Lot, A., Fa, J., Eds.; Oxford University Press: New York, NY, USA, 1993; pp. 447–458.

51. Zavala, F. Los encinos mexicanos: Un recurso desaprovechado. *Cienc. Desarro.* **1990**, *16*, 43–51.

52. Richter, G.; Fuentes, F.; Silva, J.; Rodríguez, R.; Torres, P. *Fichas de Propiedades Tecnológicas de las Maderas*; Departamento de Madera, Celulosa y Papel. CUCEI. Universidad de Guadalajara: Guadalajara, México, 2012.

53. Manos, P.S.; Doyle, J.J.; Nixon, K.C. Phylogeny, biogeography, and processes of molecular differentiation in Quercus subgenus Quercus (Fagaceae). *Mol. Phylogenet. Evol.* **1999**, *12*, 333–349. [CrossRef]

54. Arizaga, S.; Martínez-Cruz, J.; Salcedo-Cabrales, M.; Bello-González, M.A. *Manual de la Biodiversidad de Encinos Michoacanos*, 1st ed.; Instituto Nacional de Ecología: México, D.F., Mexico, 2009.

55. Morales-Saldaña, S.; Luna-Bonilla, O.Á.D.; Cadena-Rodríguez, Y.J.; Valencia, A.S. Species distribution of Quercus (Fagaceae) along an altitude gradient, reveals zonation in a hotspot. *Bot. Sci.* **2021**, *99*, 722–734. [CrossRef]

56. Nájera-Luna, J.A.; Vargas-Antonio, Z.; Méndez-González, J.; de Jesús Graciano-Luna, J. Propiedades físicas y mecánicas de la madera en Quercus laeta Liemb. de El Salto, Durango. *Ra Ximhai* **2005**, *1*, 559–576. Available online: https://www.redalyc.org/pdf/461/46110307.pdf (accessed on 10 October 2021). [CrossRef]

57. *ASTM D 638-14*; Standard Test Method for Tensile Properties of Plastics. American Society for Testing and Materials: West Conshohocken, PA, USA, 2014.

58. *ASTM D 790-15e2*; Standard Test Method for Flexural Properties of Unreinforced and Reinforced Plastics and Electrical Insulating Materials Properties. American Society for Testing and Materials: West Conshohocken, PA, USA, 2015.

59. *ASTM D 5628-96*; Standard Test Method for Impact Resistance of Flat, Rigid Plastic Specimens by Means of Falling Dart (Tup or Falling Mass). American Society for Testing and Materials: West Conshohocken, PA, USA, 1996.

60. *ASTM D1238-13*; Standard Test Method for Melt Flow Rates of Thermoplastics by Extrusion Plastometer. American Society for Testing and Materials: West Conshohocken, PA, USA, 2013.

61. Cranks, J. *The Mathematics of Diffusion*; Oxford University Press: London, UK, 1979; Chapter IV.

62. Ashori, A. Hybrid Composites from Waste Materials. *J. Polym. Environ.* **2009**, *18*, 65–70. [CrossRef]

63. Maldas, D.; Kokta, B.V.; Daneault, C. Thermoplastic composites of polystyrene: Effect of different wood species on mechanical properties. *J. Appl. Polym. Sci.* **1995**, *38*, 413–439. [CrossRef]

64. Stark, N.M.; Rowlands, R.E. Effects of wood fiber characteristics on mechanical properties of wood/polypropylene composites. *Wood Fiber Sci.* **2003**, *35*, 167–174.

65. Yang, H.S.; Kim, H.J.; Park, H.J.; Lee, B.J.; Hwang, T.S. Water absorption behavior and mechanical properties of lignocellulosic filler–polyolefin bio-composites. *Compos. Struct.* **2006**, *72*, 429–437. [CrossRef]

66. Najafi, S.K.; Sharifnia, H.; Tajvidi, M. Effects of water absorption on creep behavior of wood-plastic composites. *J. Compos. Mater.* **2008**, *42*, 993–1002. [CrossRef]

67. Mishra, S.; Verma, J. Effect of compatibilizers on water absorption kinetics of polypropylene/wood flour foamed composites. *J. Appl. Polym. Sci.* **2006**, *101*, 2530–2537. [CrossRef]

68. Tajvidi, M.; Najafi, S.K.; Moteei, N. Long-term water uptake behavior of natural fiber/polypropylene composites. *J. Appl. Polym. Sci.* **2006**, *99*, 2199–2203. [CrossRef]

69. Jawaid, M.; Khalil, H.A.; Bakar, A.A. Mechanical performance of oil palm empty fruit bunches/jute fibres reinforced epoxy hybrid composites. *Mater. Sci. Eng. A* **2010**, *527*, 7944–7949. [CrossRef]

70. Nourbakhsh, A.; Ashori, A. Fundamental studies on wood–plastic composites: Effects of fiber concentration and mixing temperature on the mechanical properties of poplar/PP composite. *Polym. Compos.* **2008**, *29*, 569–573. [CrossRef]

71. Ichazo, M.N.; Albano, C.; Gonzalez, J.; Perera, R.; Candal, A.M. Polypropylene/wood flour composites: Treatments and properties. *Compos. Struct.* **2001**, *54*, 207–214. [CrossRef]

72. Nair, K.M.; Diwan, S.M.; Thomas, S. Tensile properties of short sisal fiber reinforced polystyrene composites. *J. Appl. Polym. Sci.* **1996**, *60*, 1483–1497. [CrossRef]

73. Zhu, M.; Song, J.; Li, T.; Gong, A.; Wang, Y.; Dai, J.; Yao, Y.; Luo, W.; Henderson, D.; Hu, L. Highly anisotropic, highly transparent wood composites. *Mater. Av.* **2016**, *28*, 5181–5187. [CrossRef]

74. Borysiak, S.; Paukszta, D. Mechanical Properties of Lignocellulosic/Polypropylene Composites. *Mol. Cryst. Liq. Cryst.* **2008**, *484*, 379–388. [CrossRef]

75. Ashori, A.; Nourbakhsh, A. Reinforced polypropylene composites: Effects of chemical compositions and particle size. *Bioresour. Technol.* **2010**, *101*, 2515–2519. [CrossRef] [PubMed]